

29
NASA TN D-1626

NASA, TN D-1626



N63-13950

code-1

TECHNICAL NOTE

D-1626

EXPERIMENTAL PRESSURES AND
TURBULENT HEAT-TRANSFER COEFFICIENTS ASSOCIATED
WITH SINUSOIDAL PROTUBERANCES ON A FLAT PLATE

AT A MACH NUMBER OF 3

By Charles P. Shore, Sidney C. Dixon,
and George E. Griffith

Langley Research Center
Langley Station, Hampton, Va.

NATIONAL AERONAUTICS AND SPACE ADMINISTRATION
WASHINGTON

March 1963

554036

32p

NATIONAL AERONAUTICS AND SPACE ADMINISTRATION

TECHNICAL NOTE D-1626

EXPERIMENTAL PRESSURES AND
TURBULENT HEAT-TRANSFER COEFFICIENTS ASSOCIATED
WITH SINUSOIDAL PROTUBERANCES ON A FLAT PLATE
AT A MACH NUMBER OF 3

By Charles P. Shore, Sidney C. Dixon,
and George E. Griffith

SUMMARY

An exploratory investigation was made to determine the local effects on aerodynamic heating produced by three-dimensional sinusoidal-type skin buckles of various depths. Tests were made at a Mach number of 3.0, a stagnation pressure of 200 pounds per square inch absolute, a stagnation temperature of 500° F, and a free-stream Reynolds number per foot of approximately 14×10^6 . Temperatures were obtained from one set of test specimens and pressures from another. The test results, presented in terms of Stanton numbers and pressure coefficients, show that marked increases or decreases in aerodynamic heating and pressure can result from changes in contour produced by skin buckles.

INTRODUCTION

Analytical calculation of the heat transfer to the external skin of supersonic vehicles generally assumes that the surface is smooth and aerodynamically clean with the local flow conditions known. Such predictions may be invalidated by changes in the local flow characteristics resulting from surface protuberances or thermally induced buckles and distortions in the outer skin surface. (See, for example, refs. 1, 2, and 3.) In the severe thermal environment of hypervelocity flight, the design and choice of material for structural surfaces may be dependent on an accurate assessment of local heating rates. Thus, knowledge of surface contour effects on local heating rates is desirable.

Consequently, an exploratory experimental investigation was conducted to ascertain variations in local heating rates over various skin-buckling shapes. The investigation was conducted at a Mach number of 3.0 in the Langley 9- by 6-foot thermal structures tunnel on three-dimensional sinusoidal buckle shapes impressed to various depths in aluminum-alloy panels. Temperatures and pressures over the panels were measured at essentially constant values of stagnation temperature and pressure of 500° F and 200 pounds per square inch absolute, respectively. These

conditions correspond to a free-stream Reynolds number per foot of about 14×10^6 and produced a calculated turbulent boundary-layer velocity thickness of approximately 0.43 inch (see ref. 4) and a Reynolds number of about 48×10^6 at the leading edge of the buckles.

SYMBOLS

C_p	pressure coefficient, $\frac{P_s - P_\infty}{q_\infty}$
c	specific heat of material, $\frac{\text{Btu}}{\text{lb-}^\circ\text{F}}$
c_p	specific heat of air at constant pressure, $\frac{\text{Btu}}{\text{slug-}^\circ\text{F}}$
h	aerodynamic heat-transfer coefficient, $\frac{\text{Btu}}{\text{ft}^2\text{-sec-}^\circ\text{F}}$
h_b	buckle depth, in.
l	buckle length, in.
m	density of panel material, lb/cu ft
N_{St}	Stanton number, $h/c_p\rho V$
p	pressure, lb/sq in. abs
q	dynamic pressure, $\frac{1}{2}\rho V^2$, lb/sq in. abs
T	temperature, $^\circ\text{F}$
T_{aw}	adiabatic wall temperature, $^\circ\text{F}$
t	time, sec
V	air velocity, ft/sec
x	distance from leading edge of panel, in.
ρ	density of air, slug/cu ft
τ	skin thickness, ft

Subscripts:

s local static conditions

t	stagnation conditions
∞	free-stream conditions
ref	flat reference panel
max	maximum
eq	equilibrium

PANELS, APPARATUS, AND TESTS

Panels

The test specimens were 10 inches wide and 29 inches long and were made from 0.375-inch-thick aluminum-alloy plates. To obtain the desired panel configurations the aluminum-alloy plates were chemically milled to within a few thousandths of the desired final skin thickness of 0.080 inch. The resulting panels were then machined to final dimensions and stamped to the desired buckle shape. (See figs. 1 to 3 for typical panel construction details and photographs of a panel in various stages of development.) As shown in figures 1 to 3, the panels were integrally stiffened around the buckled area to prevent thermal buckling of the flat portions of the panels and aid in preventing undesired distortions while the buckles were being formed. The buckle pattern consisted of either a single buckle extending into or away from the flow or a double buckle, one into and one away from the flow. The cross section of the buckles was essentially that of a half sine wave; the buckles had depths up to 0.851 inch and nominal lengths of 6 inches except for one panel with a single buckle 4 inches long. For all panels, the distance from the leading edge of the panel to the leading edge of the buckle was maintained constant at approximately 14 inches. For the purpose of obtaining pressure data, duplicates were made of four of the original nine panels (designated by affixing A to the panel number); however, the contours of the buckles did not identically match those of the original panels. A single flat panel was used as a reference panel for obtaining both temperatures and pressures and checking flow conditions.

The various panel configurations are illustrated in figure 4. The actual shape of the buckles was determined by measuring the vertical distance from the plane of the flat surface of the panel to various points along the center line of a buckle with the aid of a precision jig borer; the flat surface exposed to the air flow was used as the reference plane. The resulting measurements are given in table I.

Instrumentation

The panels used to obtain temperature data were instrumented with from 20 to 30 iron-constantan thermocouples spotwelded to the inner skin surface principally along the longitudinal center line, and 3 or 4 pressure orifices; the pressure panels had 19 pressure orifices and no thermocouples. Instrumentation location

is shown in figure 5. The malfunction of some thermocouples resulted in the necessity of retesting panels 2, 4, 5, 6, and 7. For these tests, additional thermocouples were added along the longitudinal center line of the buckles such that the thermocouple spacing over the buckles was a half inch. All data were recorded either on magnetic tape or oscillograph records.

Test Apparatus

Langley 9- by 6-foot thermal structures tunnel.- All tests were conducted in the Langley 9- by 6-foot thermal structures tunnel, an intermittent blowdown facility operating at a Mach number of 3.0 and exhausting to the atmosphere. A heat exchanger is preheated to provide stagnation temperatures up to 660° F. During tunnel starting and shutdown, the flow separates from the nozzle walls with the result that unprotected specimens are buffeted by rough air flow and are subjected to loads considerably in excess of those applied during the period of test conditions. (See ref. 5 for additional details regarding the tunnel.)

Panel holder and mounting arrangement.- The panels were mounted in a panel holder which extended vertically through the test section. (See fig. 6.) The panel holder has a beveled half-wedge leading edge, flat sides, and a recess 29 inches wide and 30 inches high for accommodating test specimens; the recess is located on the nonbeveled side of the panel holder 26.5 inches downstream of the leading edge. Pneumatically operated sliding doors protect test specimens from aerodynamic buffeting and heating during tunnel starting and shutdown. Aerodynamic fences prevent shock waves emanating from the doors from interfering with the air flow over the test specimens. The average flow conditions over the area of recess, determined from pressure surveys of a flat calibration panel (ref. 5) and checked by data from the flat reference panel, were essentially free-stream conditions. However, there were some variations in the local flow conditions near the outer edges of the recess.

Test Conditions

The panels were mounted three at a time (consisting of the flat reference panel and two buckled panels) in the panel holder so that the flat portion of the models was flush with the flat side of the panel holder and the longitudinal edges were parallel to the direction of air flow. (See fig. 6(b).) The panel holder was at zero angle of attack for the tests. All tests were conducted at a Mach number of 3.0 and at essentially constant stagnation temperatures and pressures of approximately 500° F and 200 pounds per square inch absolute, respectively. Based on the distance from the leading edge of the panel holder, these conditions produced a calculated (see ref. 4) turbulent boundary-layer velocity thickness of about 0.43 inch and a free-stream Reynolds number of about 48×10^6 at the leading edge of the buckles. Figure 7 shows the variation of tunnel stagnation temperature and pressure during a typical test. The protective doors were opened about 3 seconds after the start of air flow (time to fully open doors is approximately 0.5 second) and were closed about 3 seconds before tunnel shutdown. Test conditions lasted approximately 20 seconds.

DATA REDUCTION

Pressures

The measured pressures were converted to dimensionless pressure coefficients of the usual form

$$C_p = \frac{p_s - p_\infty}{q_\infty} \quad (1)$$

where p_s was the actual measured local panel pressure; the free-stream static pressure p_∞ was obtained from previously determined experimental data for a flat calibration panel (ref. 5) and checked by data from the reference panel.

Heat-Transfer Coefficients

If radiation and conduction losses can be ignored and the temperature gradient through the thickness is unimportant, the differential equation describing the heat balance of an element of exposed skin of constant thickness subjected to aerodynamic heating is

$$h(T_{aw} - T) = cm\tau \frac{dT}{dt} \quad (2)$$

Equation (2) can be rearranged as

$$T = - \frac{cm\tau}{h} \frac{dT}{dt} + T_{aw} \quad (3)$$

which, if c , m , τ , h , and T_{aw} are assumed to be constant, is the equation of a straight line in T and dT/dt where h can be determined from the slope and T_{aw} is the T -axis intercept at $dT/dt = 0$. The data were reduced to heat-transfer coefficients by graphic solution of equation (3) as illustrated in figures 8(a) and 8(b) for a typical set of test data. The slope of the temperature variation with time was obtained at various intervals along the curve. (See fig. 8(a).) Values of the temperature T were then plotted as functions of these slopes dT/dt and a straight line faired through the data points. (See fig. 8(b).) The slope $\frac{\Delta T}{\Delta \frac{dT}{dt}}$ of this straight line yields values of h for the

time period considered. The method neglects the effects of small variations in test conditions and the previously mentioned radiation and conduction effects. Thus, the values of h obtained from the graphic solution are not the actual experimental values and the value of the T -axis intercept is actually an equilibrium temperature T_{eq} rather than the true T_{aw} . However, since the primary

intent of this investigation was to determine trends in the h-distribution, these effects were considered insufficient to alter the results greatly.

Conversion of heat-transfer coefficients to dimensionless Stanton numbers was accomplished by using the well-known definition

$$N_{St} = \frac{h}{c_{p,\infty} \rho_{\infty} V_{\infty}} \quad (4)$$

where h is the local value of the heat-transfer coefficient and $c_{p,\infty}$, ρ_{∞} , and V_{∞} are free-stream values.

RESULTS AND DISCUSSION

Pressures

Results are presented for only three of the four pressure panels. (See fig. 5.) The fourth panel (panel 3A), which had a 0.851-inch buckle directed away from the flow, was tested twice. Early in the first test of panel 3A a malfunctioning of the data-transmission circuits occurred; however, prior to this time the data appeared to be both varying and inconsistent. During a later test the data appeared to be very erratic and without trend; hence the results for panel 3A are not presented. However, it is not known whether the recorded data were inaccurate or whether unsteady flow separation occurred as a result of the shape and depth of the depression.

Results in the form of pressure coefficients are presented for the other three pressure panels (panels 2A, 8A, and 9A) in figure 9. The solid lines represent curves arbitrarily drawn through the test points obtained along the center line of the panel. The dashed lines represent theoretical values of C_p based on calculations using two-dimensional small perturbation theory (see ref. 6); pertinent center-line buckled deflections are shown in table I.

The agreement between the measured variation and the theoretical variation is surprisingly good. However, the maximum experimental value of the pressure coefficient on the compressive face of the buckles is generally somewhat less than theory (because of three-dimensional effects), but appears to be linearly related to the depth of the contour. Also, as indicated by the double-buckle contours, the magnitude of the pressure coefficient does not appear to depend on the buckle sequence. The minimum values of C_p on the expansion faces were reasonably close to the theoretical values. The close proximity of the measured data points to the theoretical variation for the panels shown suggests that flow separation probably did not occur for any of the panels tested.

As mentioned in the section entitled "Panels," the contours of the pressure panels did not duplicate those of the heat-transfer panels because of fabrication difficulties. These differences in contour were considered sufficient to alter

the flow conditions to an extent which precluded the use of the pressure data for establishing accurate local conditions for the heat-transfer panels; however, the difference in contour were considered insufficient to invalidate the conclusion that flow separation probably did not occur for the heat-transfer panels.

Heat-Transfer Coefficients

The aerodynamic heat-transfer coefficients are presented in the form of Stanton numbers for several panels in figure 10. The solid lines represent arbitrary curves faired through the experimental data for the buckled panels, the long dashed lines represent experimental values of the Stanton number for the flat reference panel, and the short dashed lines represent theoretical values of the Stanton number for the flat reference panel based on theoretical values of h . Theoretical values of h were obtained from the turbulent-flow flat-plate theory presented in reference 7 by using initial free-stream flow conditions and a skin temperature equal to the panel temperature at initial exposure to the flow. Experimental values of h for the flat reference panel always were within 5 percent of those obtained by the theoretical calculations.

Examination of figures 10(a) to 10(d) $\left(\frac{h_{b,max}}{\lambda} = 0.09 \right)$ reveals that for a given buckle an increase in heat-transfer coefficient (or Stanton number) results from an increase in slope, and likewise a decrease in slope reduces the heat-transfer coefficient. As was the case for the pressure coefficients, with respect to the flat reference panel, the magnitude of increase in Stanton number always considerably exceeded the magnitude of the decrease. Additionally, the magnitude of the maximum and minimum values of the Stanton number did not appear to be dependent on the buckle sequence (in-out or out-in) or on the number of buckles. However, as shown in figure 11, variation of the buckle size from $\frac{h_{b,max}}{\lambda}$ of 0.051 to 0.110 revealed that the maximum and minimum values of the Stanton number are strongly dependent on buckle size. Furthermore, the data indicate that in the region of the buckles the net heating rate per unit area is considerably increased over that of a flat plate. The upstream values of the Stanton number were essentially equal to those of the reference panel; however, because of the slightly higher pressures downstream of the buckles (see fig. 9(a)), the values of the Stanton number in this region were higher than those of the reference panel.

Since the peak values of the pressure coefficient appeared to be linearly related to the size of the buckle, it might be expected that the peak values of the Stanton number would also vary linearly with buckle size. Figure 12, which is a correlation plot for the single buckle panels, shows the variation of the peak values of the Stanton number with buckle size. The data are presented in terms of the nondimensional ratio of maximum or minimum peak values of the Stanton number to reference Stanton numbers plotted against the nondimensional ratio of

$h_{b,max}$ to λ . Only the minimum value is shown for panel 3 $\left(\frac{h_{b,max}}{\lambda} = 0.136 \right)$

because of loss of instrumentation in the region where the maximum value of the Stanton number would have occurred. The data indicate that, for the given values

of $h_{b,max}$ and l and the test conditions of this investigation, the variation in peak values of the Stanton number with buckle size is approximately linear. Furthermore, the data indicate that a relatively small buckle ($\frac{h_{b,max}}{l} = 0.05$) can increase the value of the Stanton number to a value 150 percent of the flat reference value.

CONCLUSIONS

An exploratory investigation was made to determine the local effects on aerodynamic heating produced by three-dimensional sinusoidal-type skin buckles of various depths. The tests were conducted at a Mach number of 3.0, a stagnation pressure of 200 pounds per square inch absolute, a stagnation temperature of 500° F, and a free-stream Reynolds number per foot of about 14×10^6 . The center-line pressure-coefficient distributions indicated that flow separation probably did not occur during the tests. The test results, presented in the form of Stanton numbers uncorrected for conduction effects, revealed the following:

1. A variation of local slope due to the presence of skin buckles is accompanied by a similar variation in Stanton numbers, that is, an increase in slope produces an increase in Stanton number and a decrease in slope produces a decrease in Stanton number. For a given buckle the magnitude of the increase in Stanton number always exceeded the magnitude of the decrease.

2. The presence of skin buckles on a flat plate results in a net increase in the heating rate per unit area over the surface of the buckles.

3. For the results of this investigation the variation in the maximum increase or decrease in Stanton number is approximately linear with respect to the buckle depth-length ratio, but appears independent of buckle sequence and number of buckles.

4. The smallest buckle investigated (depth-length ratio of 0.05) increased the Stanton number to a value 150 percent of the flat reference value.

Langley Research Center,
National Aeronautics and Space Administration,
Langley Station, Hampton, Va., January 22, 1963.

REFERENCES

1. Burbank, Paige B., and Strass, H. Kurt: Heat Transfer to Surfaces and Pro-tuberances in a Supersonic Turbulent Boundary Layer. NACA RM L58E01a, 1958.
2. Bertram, M. H., and Wiggs, M. Margarette: Effect of Surface Distortions on the Heat Transfer to a Wing at Hypersonic Speeds. Paper No. 62-127, Inst. Aerospace Sci., June 1962.
3. Carter, Howard S.: Effect of Some External Crosswise Stiffeners on the Heat Transfer and Pressure Distribution on a Flat Plate at Mach Numbers of 0.77, 1.39, and 1.98. NACA TN 4333, 1958.
4. Schlichting, Hermann (J. Kestin, trans.): Boundary Layer Theory. McGraw-Hill Book Co., Inc., 1955.
5. Dixon, Sidney C., Griffith, George E., and Bohon, Herman L.: Experimental Investigation at Mach Number 3.0 of the Effects of Thermal Stress and Buckling on the Flutter of Four-Bay Aluminum Alloy Panels with Length-Width Ratios of 10. NASA TN D-921, 1961.
6. Staff of the Ames 1- by 3-Foot Supersonic Wind-Tunnel Section: Notes and Tables for Use in the Analysis of Supersonic Flow. NACA TN 1428, 1947.
7. Lee, Dorothy B., and Faget, Maxime A.: Charts Adapted From Van Driest's Turbulent Flat-Plate Theory For Determining Values of Turbulent Aerodynamic Friction and Heat-Transfer Coefficients. NACA TN 3811, 1956.

TABLE I.- CENTER-LINE BUCKLE MEASUREMENTS

Panel	Depth, h_b , in. for x of -														
	13	14	15	16	17	18	19	20	21	22	23	24	25	26	27
2	0.047	0.171	0.365	0.639	0.763	0.632	0.354	0.152	0.019						
2A	-.011	.016	.317	.649	.771	.630	.285	-.014	-.017						
3	-.017	-.044	-.366	-.702	-.842	-.705	-.363	-.024	-.002						
3A	-.004	-.037	-.371	-.711	-.851	-.707	-.362	-.022	-.001						
4	-.007	.016	.203	.441	.568	.428	.190	.002	-.011						
5	-.005	-.030	-.233	-.509	-.636	-.474	-.213	-.023	-.006						
6	.000	.015	.084	.189	.258	.173	.076	.012	.006						
7	-.005	.027	.252	.400	.288	.016	-.002								
8	-.008	.042	-.256	-.508	-.617	-.463	-.208	.007	.207	0.458	0.579	0.436	0.192	0.000	-0.021
8A	.000	-.028	-.182	-.386	-.496	-.350	-.161	-.032	.120	.350	.551	.508	.278	.076	-.015
9	-.007	.018	.186	.401	.490	.336	.146	-.002	-.167	-.380	-.490	-.350	-.160	-.016	.001
9A	-.009	.017	.181	.394	.482	.326	.135	-.009	-.181	-.395	-.499	-.349	-.160	-.018	-.001

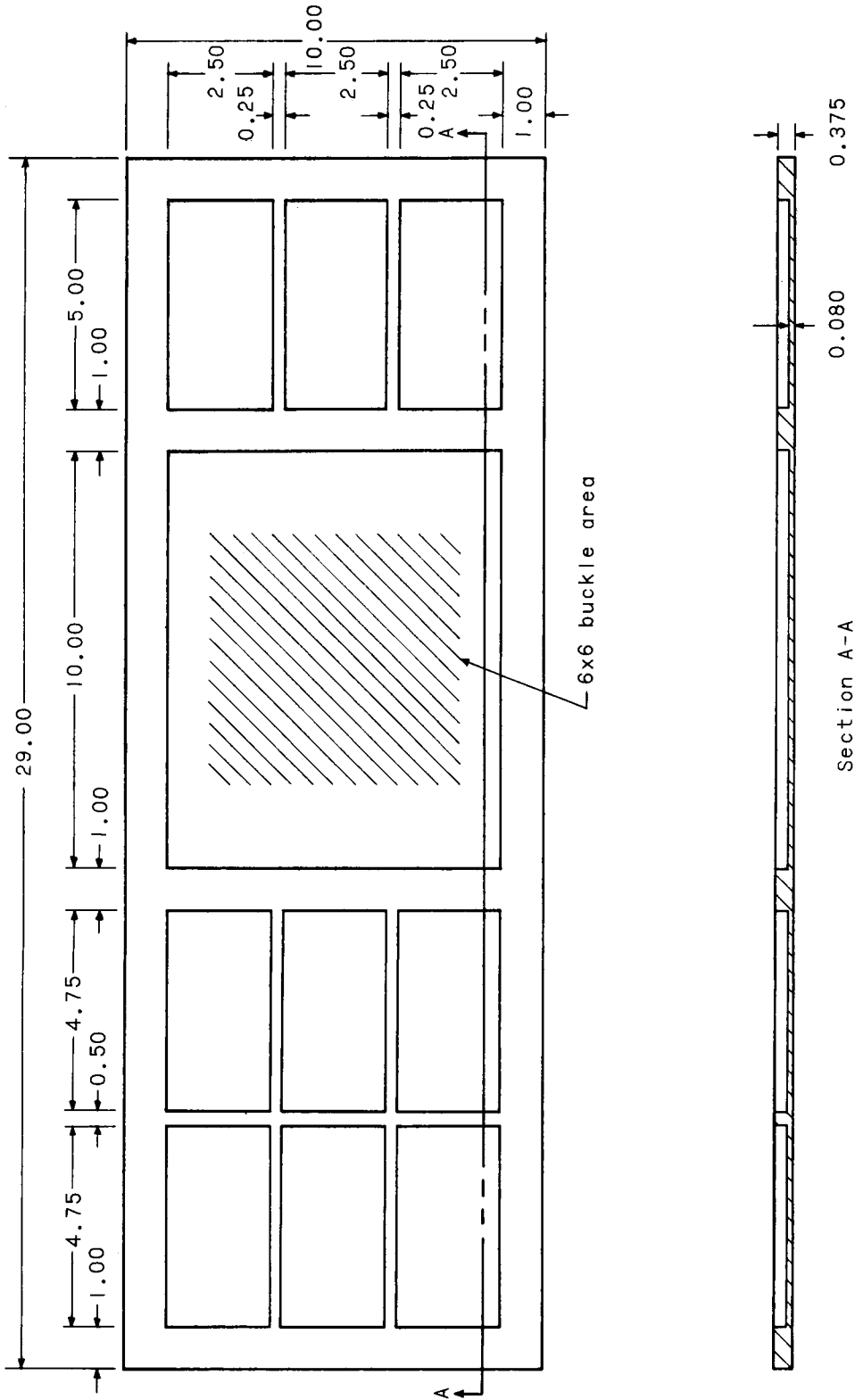


Figure 1.- Construction details (typical for 6-inch buckles) for panel 2. All dimensions are in inches.

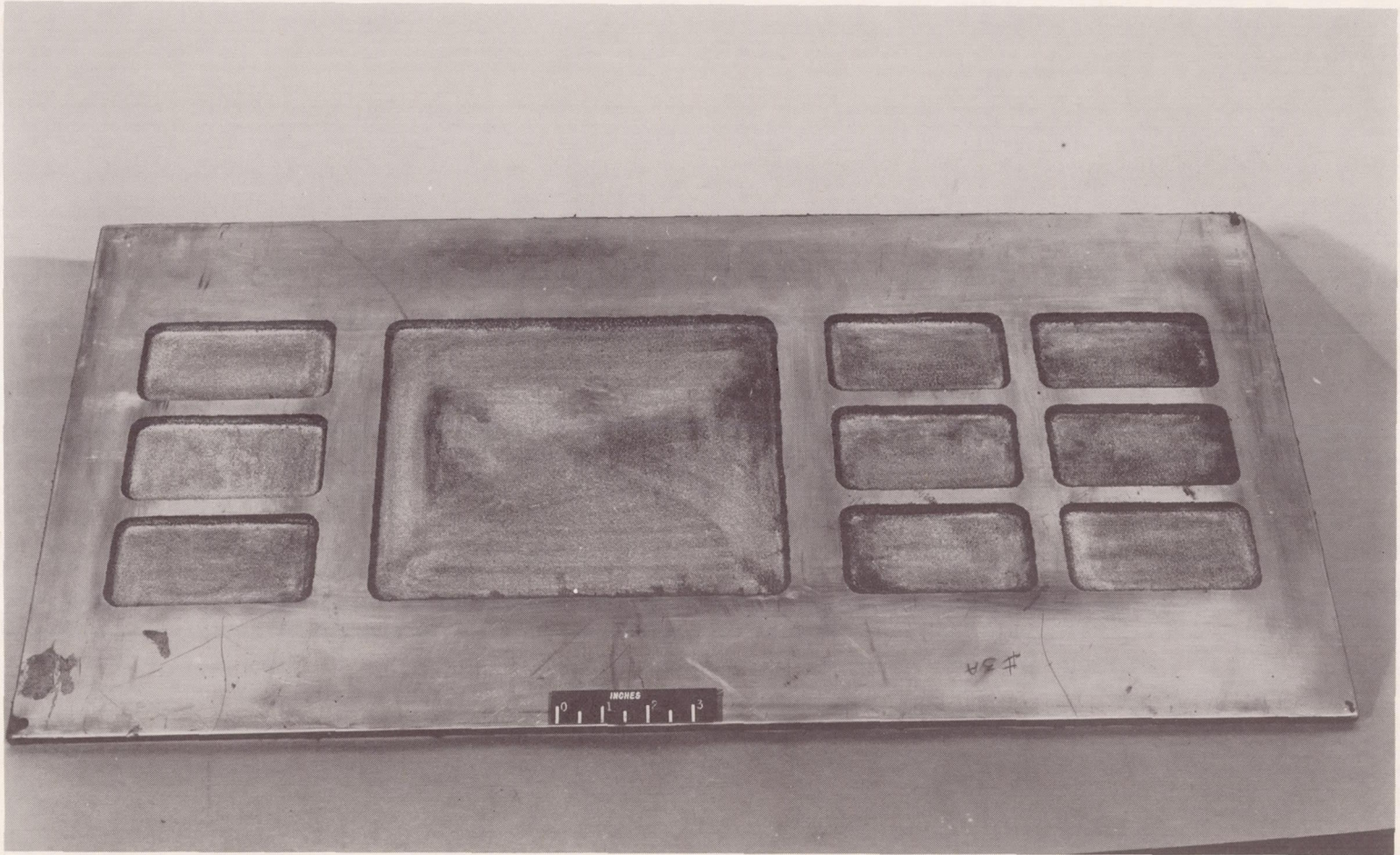


Figure 2.- Oversize 3/8-inch-thick plate after being chemically milled and ready for final machining.

L-59-5356

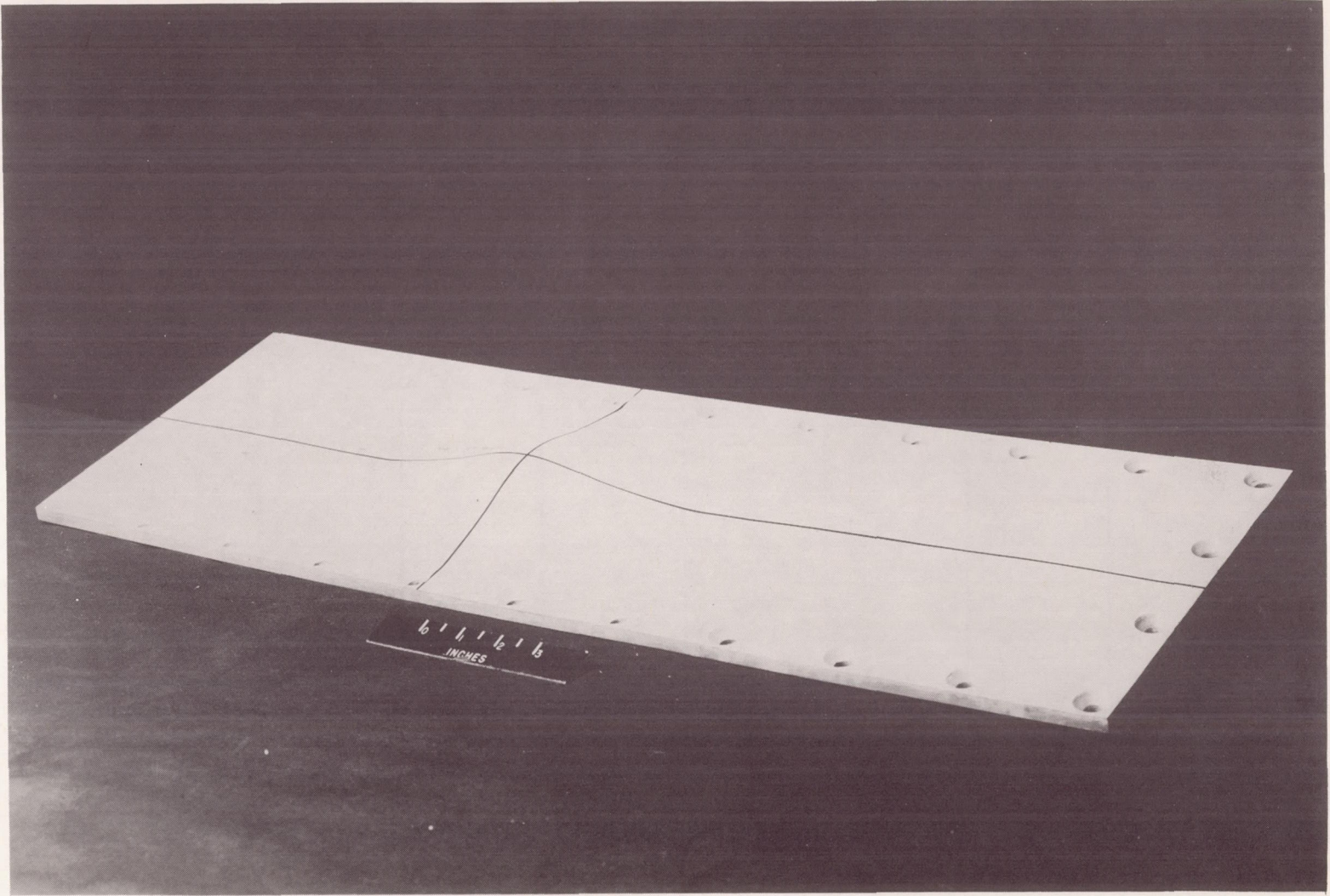


Figure 3.- Panel ready to test. (Leading edge is at right.)

L-61-5227

Panel number

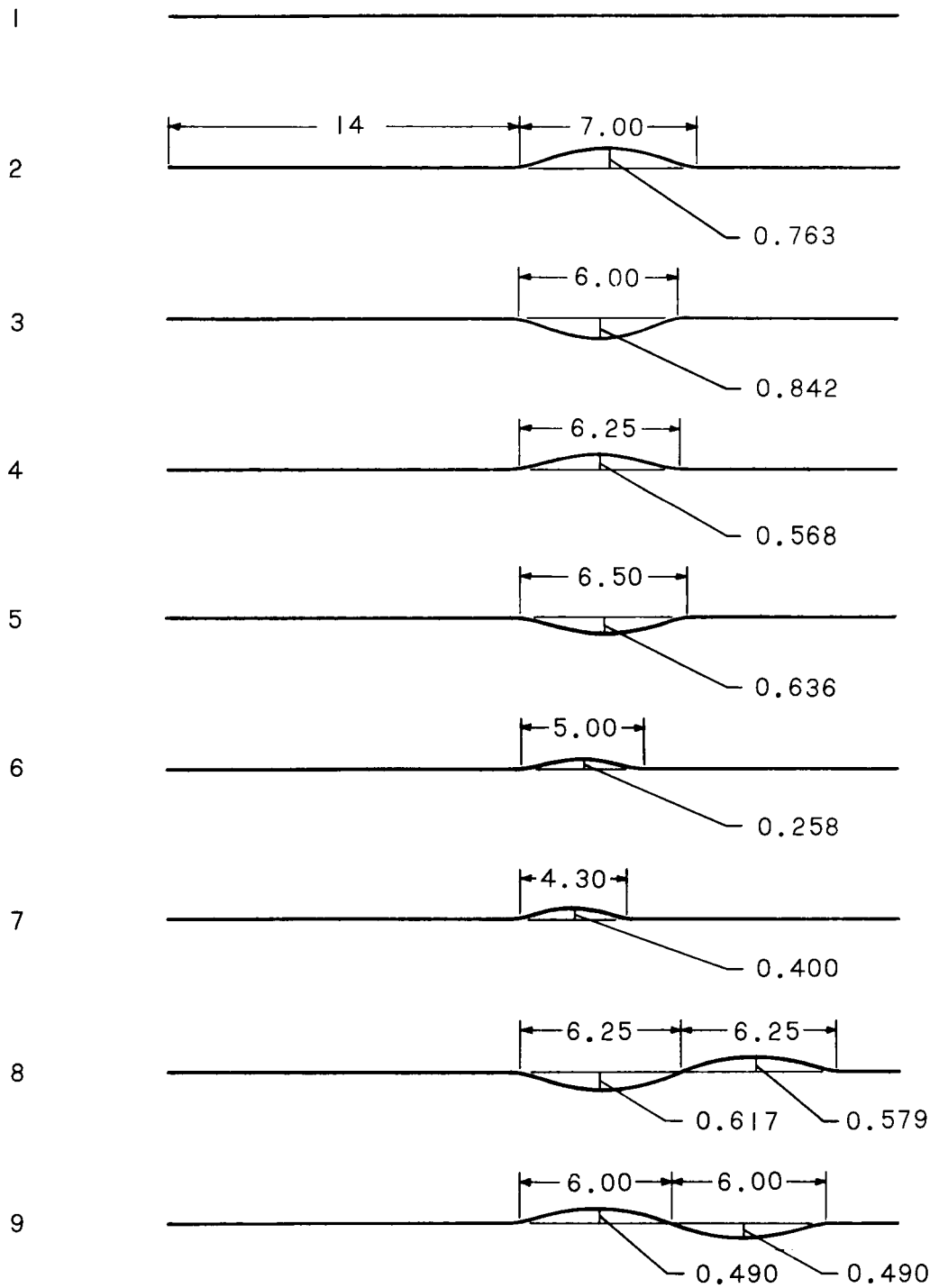
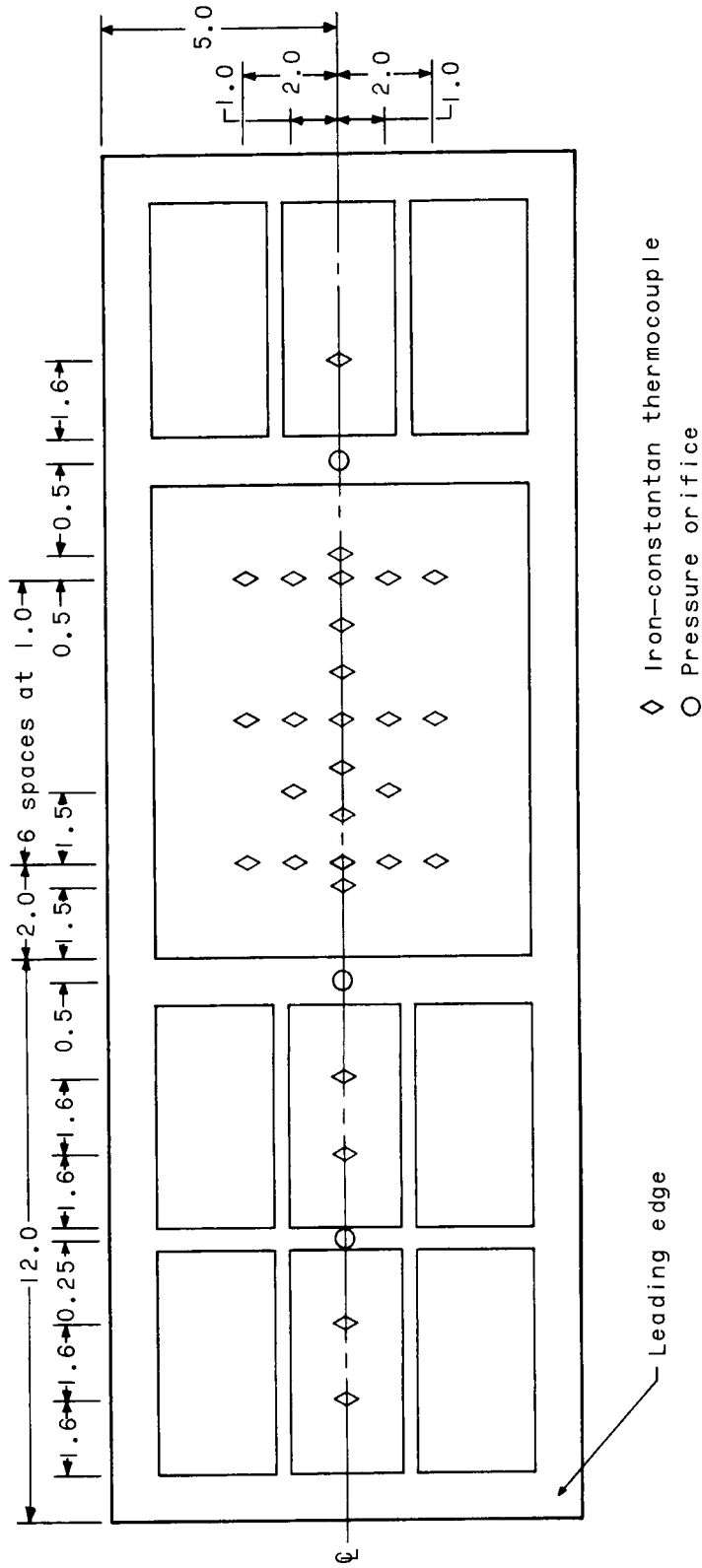
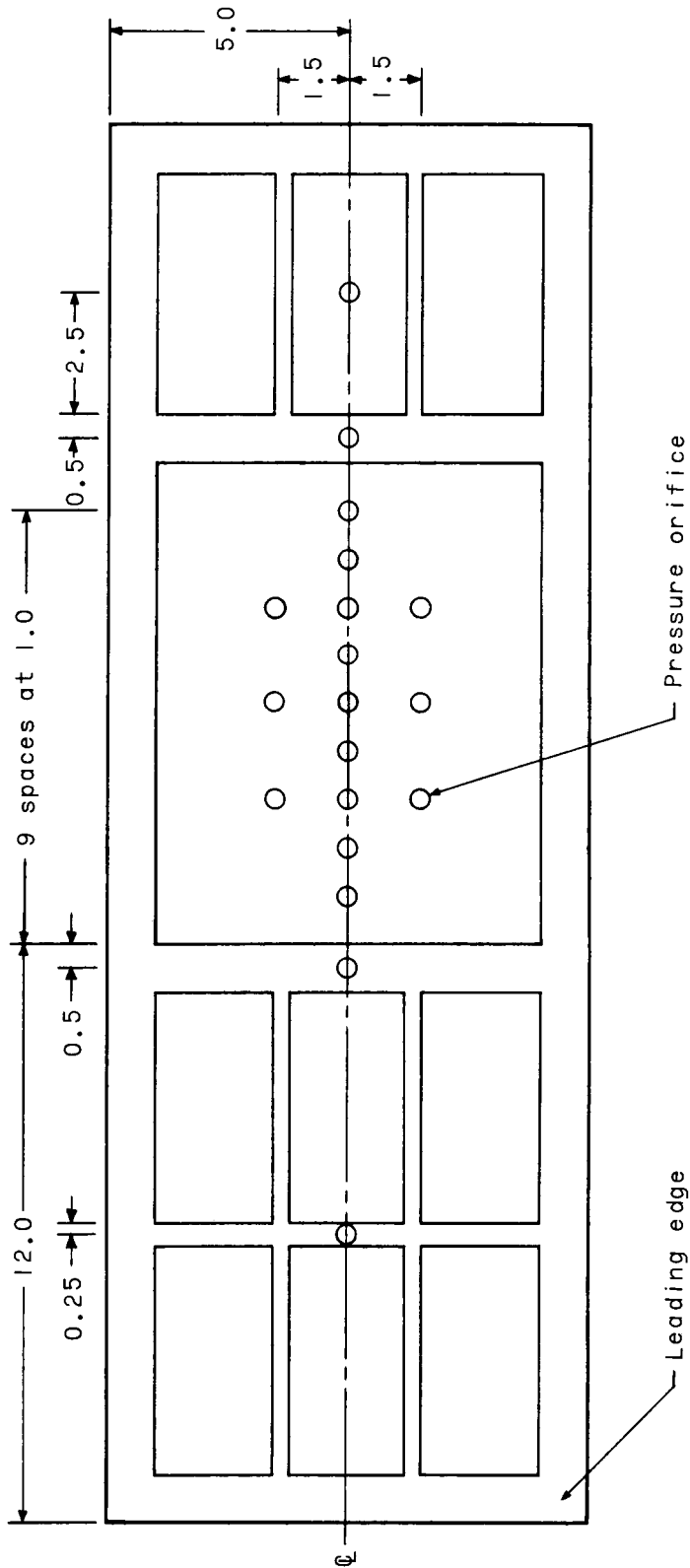


Figure 4.- Panel configurations. All dimensions are in inches.

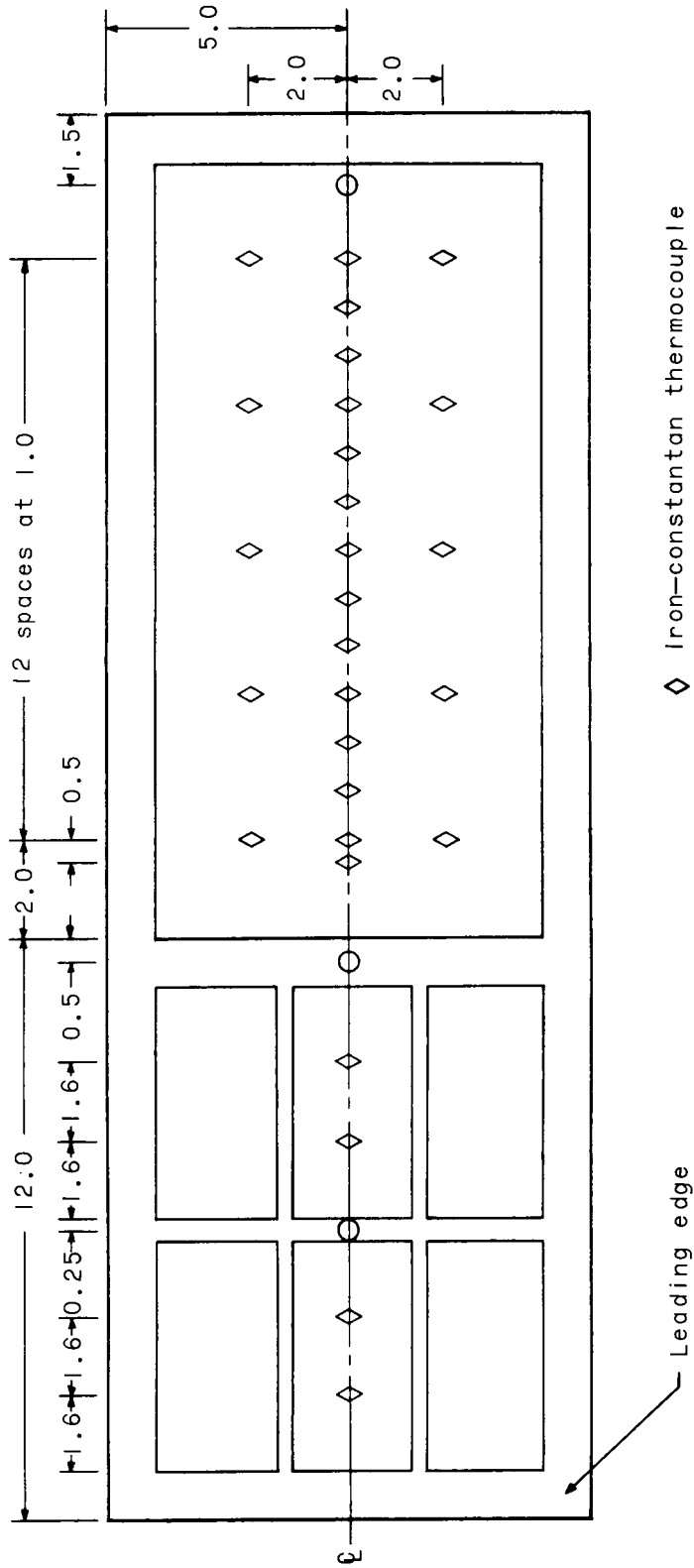


(a) 6-inch buckle temperature panel. (Panels 2, 3, 4, 5, and 6.)
 Figure 5.- Panel instrumentation. All dimensions are in inches.



(b) 6-inch buckle pressure panel. (Panels 2A and 3A.)

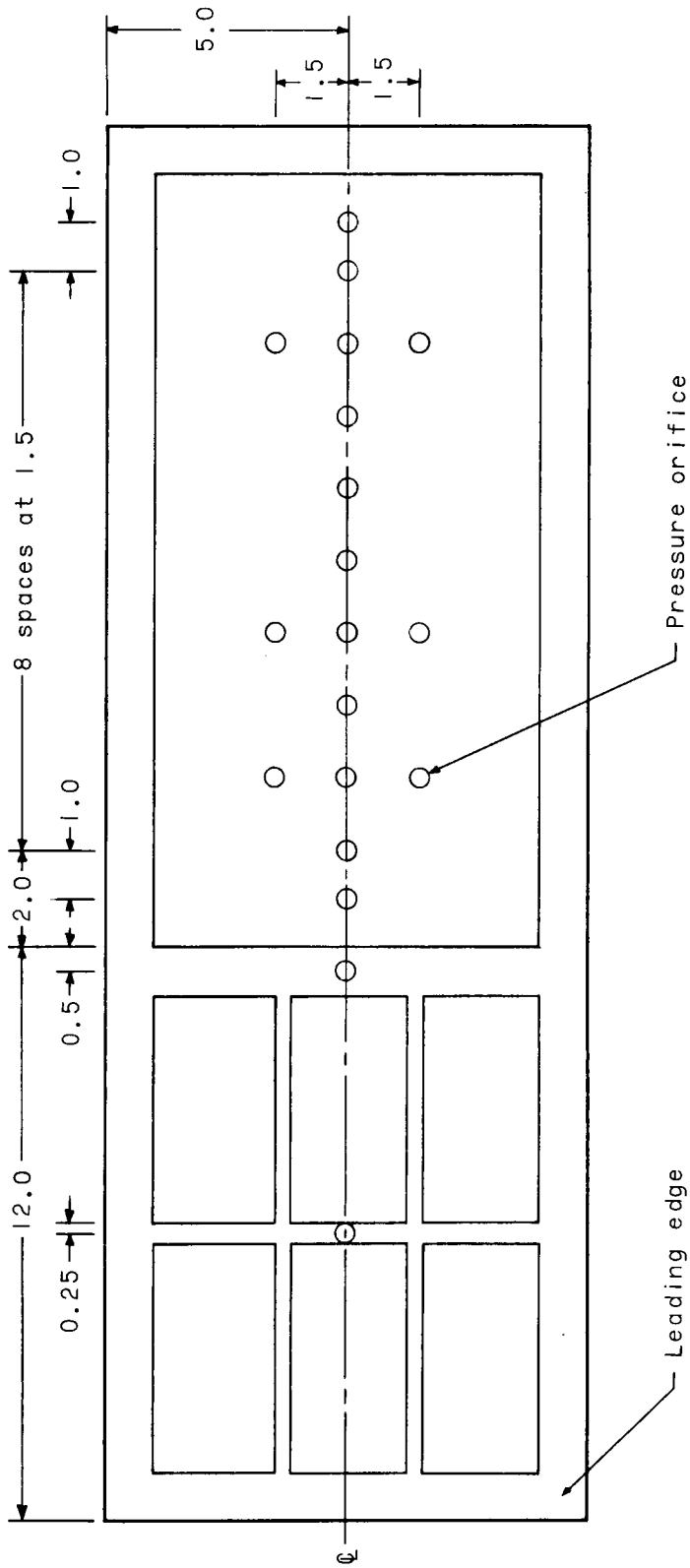
Figure 5.- Continued.



- ◇ Iron-constantan thermocouple
- Pressure orifice

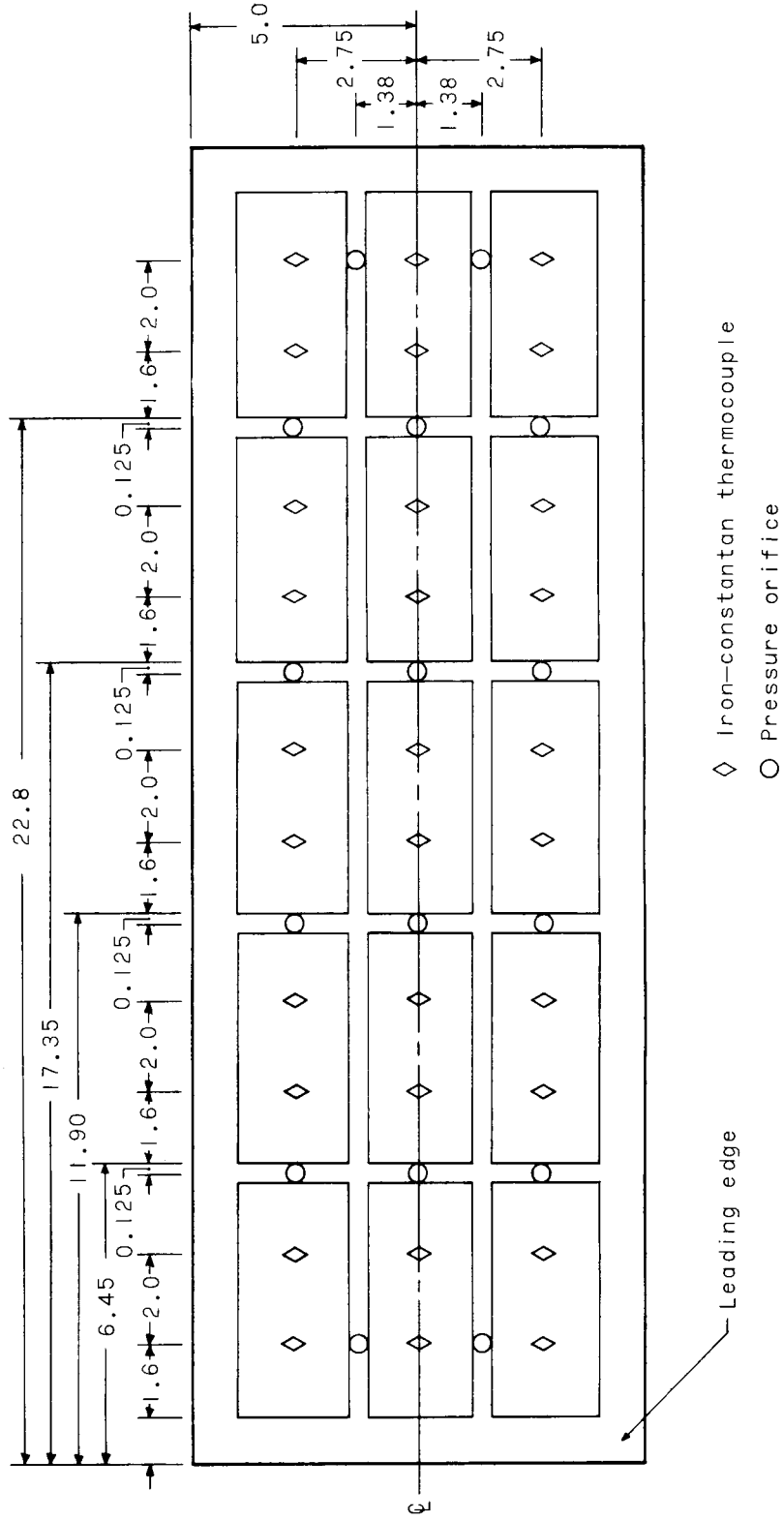
(d) Double buckle temperature panel. (Panels 8 and 9.)

Figure 5.- Continued.



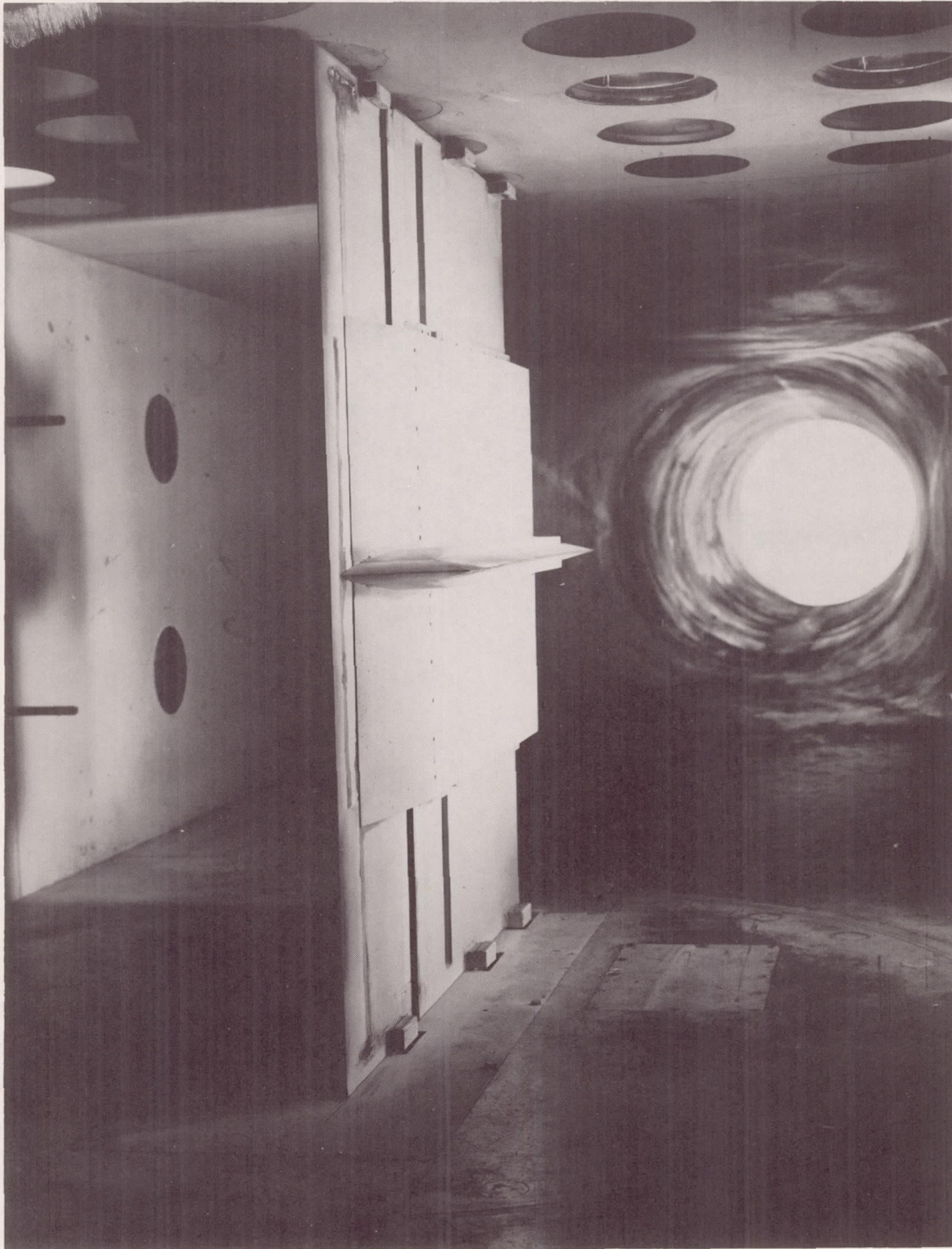
(e) Double buckle pressure panel. (Panels 8A and 9A.)

Figure 5.- Continued.



(f) Reference panel. (Panel 1.)

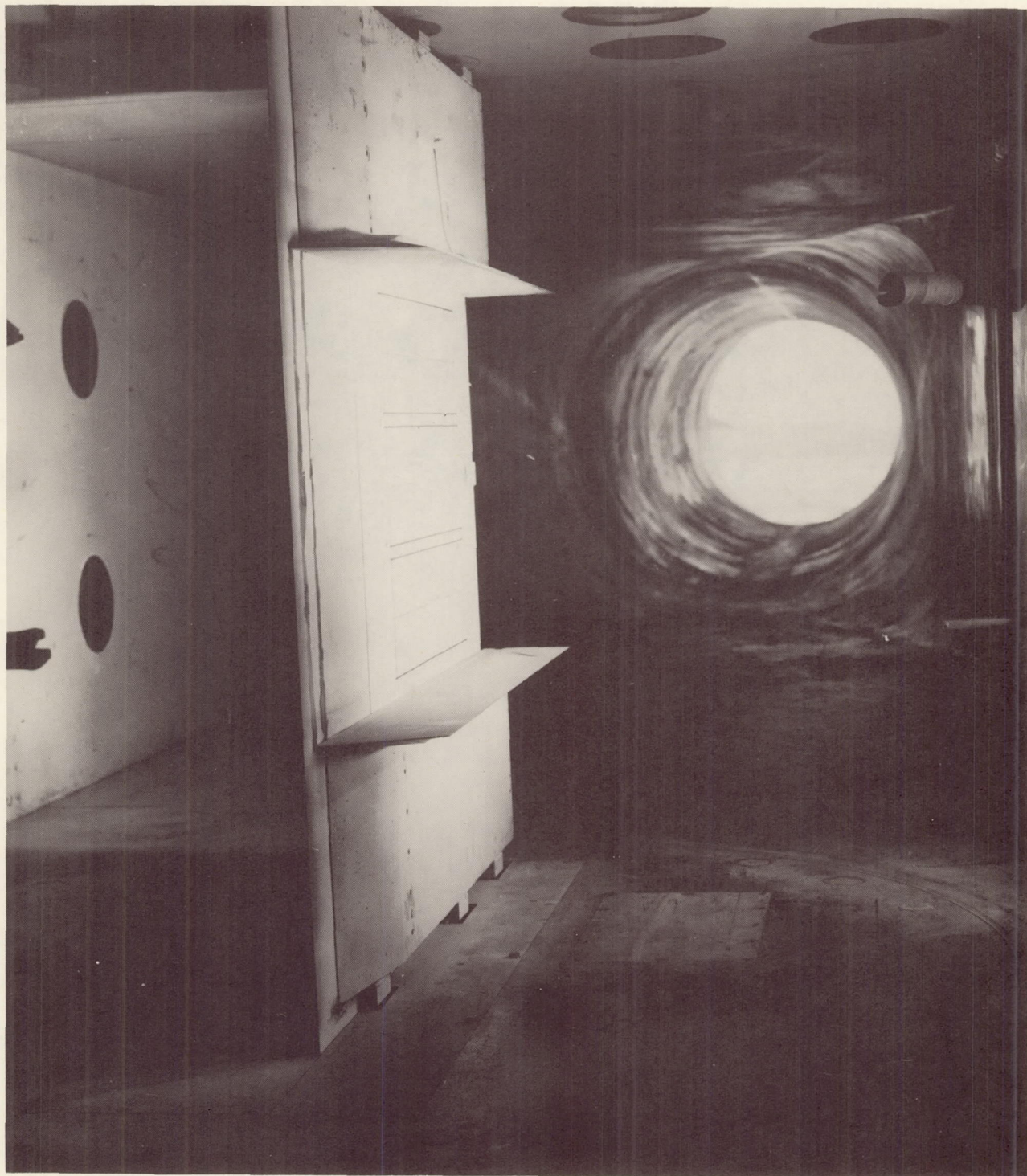
Figure 5.- Concluded.



(a) Doors closed.

L-60-5792

Figure 6.- Panel holder mounted in test section as viewed from upstream.



(b) Doors open; panels in exposed position.

L-60-5788

Figure 6.- Concluded.

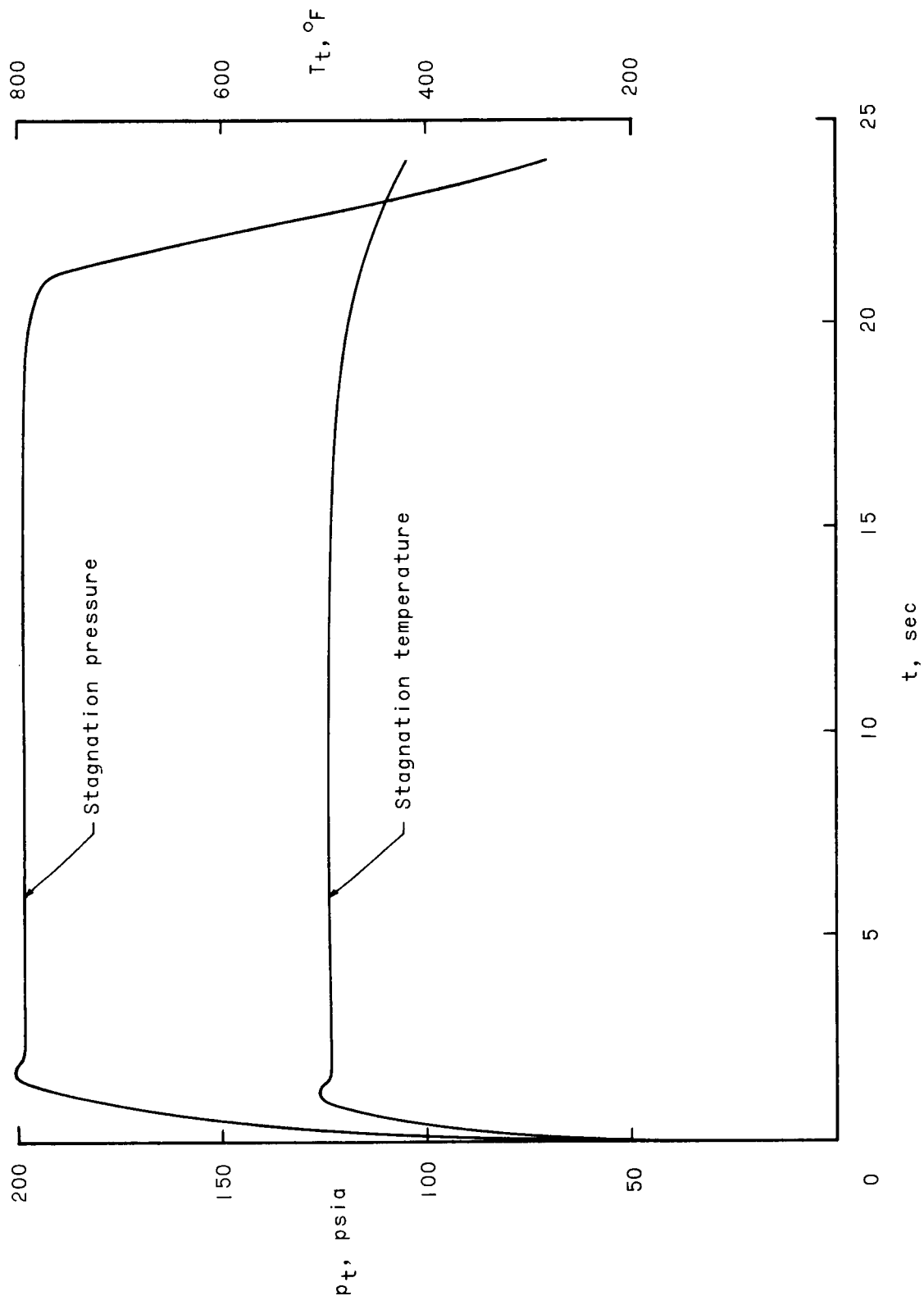
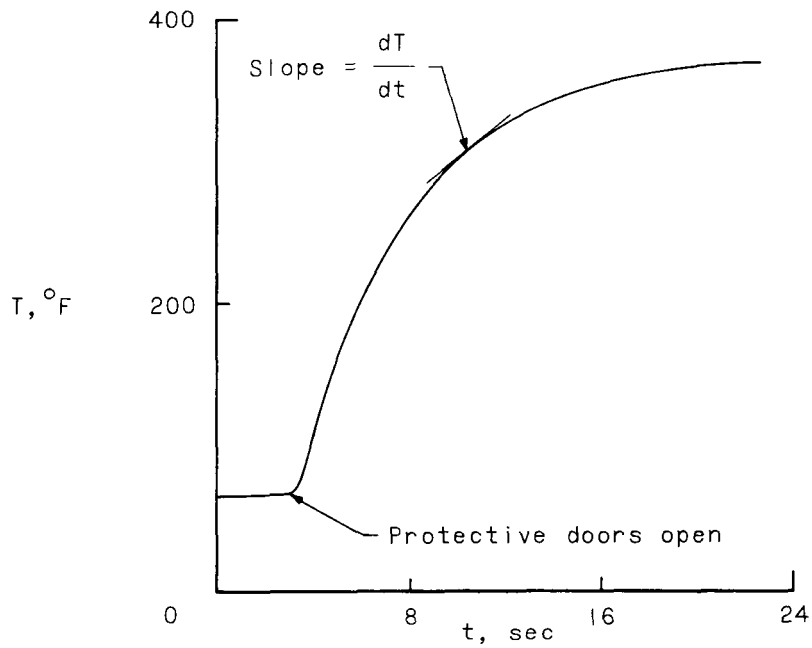
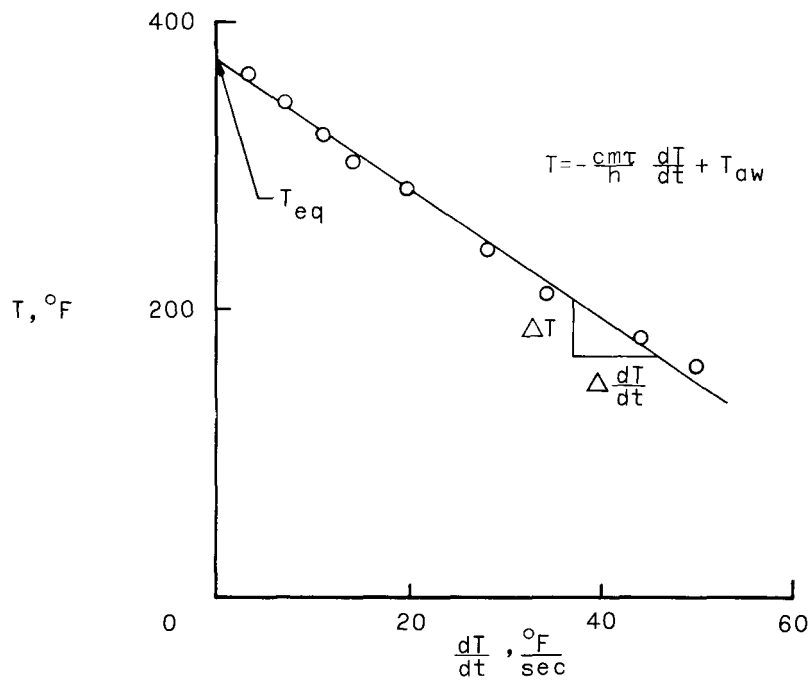


Figure 7.- Variation with time of stagnation temperature and pressure typical of all tests.

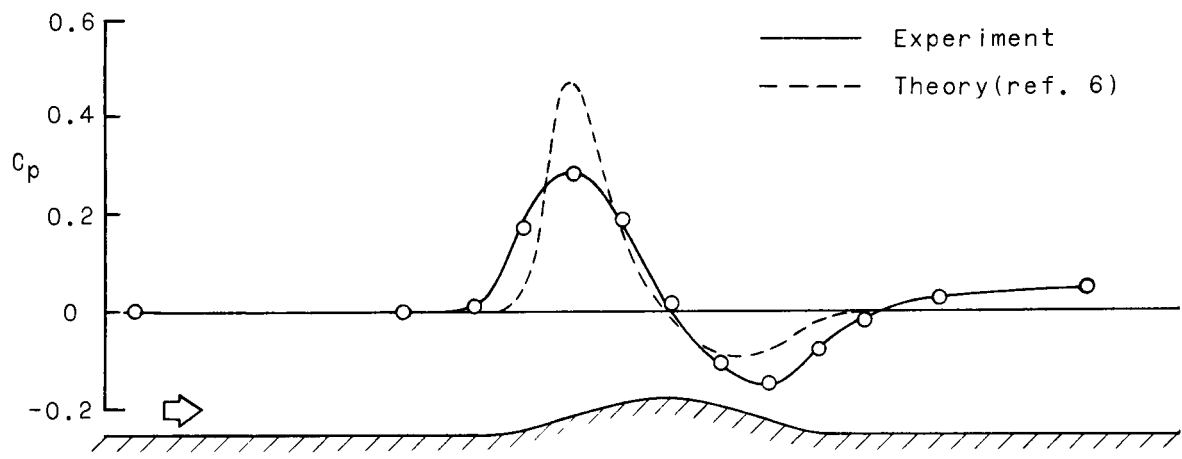


(a) Temperature history.

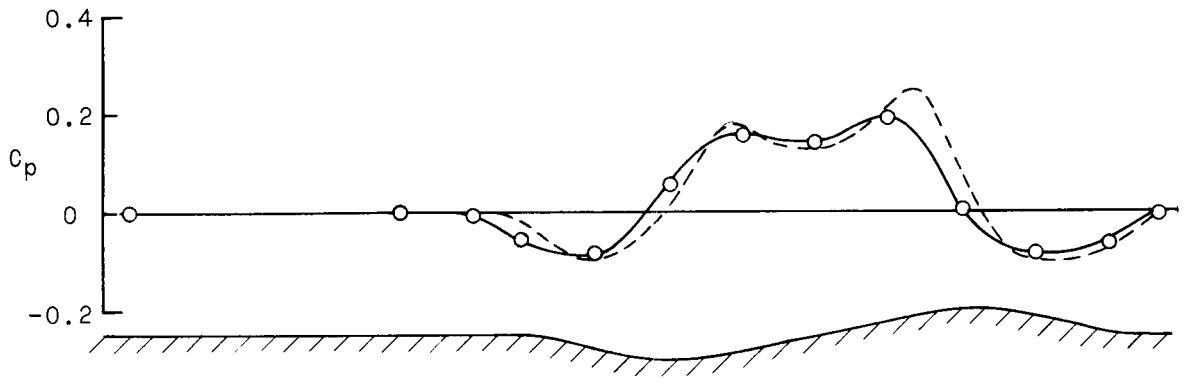


(b) Variation of temperature with dT/dt .

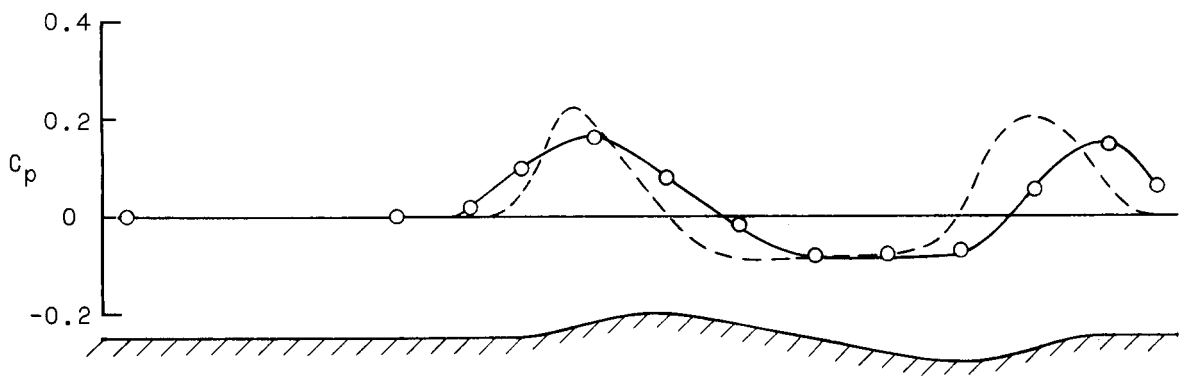
Figure 8.- Illustration of graphic solution of heat-balance equation used to obtain heat-transfer coefficients from measured temperatures.



(a) Panel 2A.

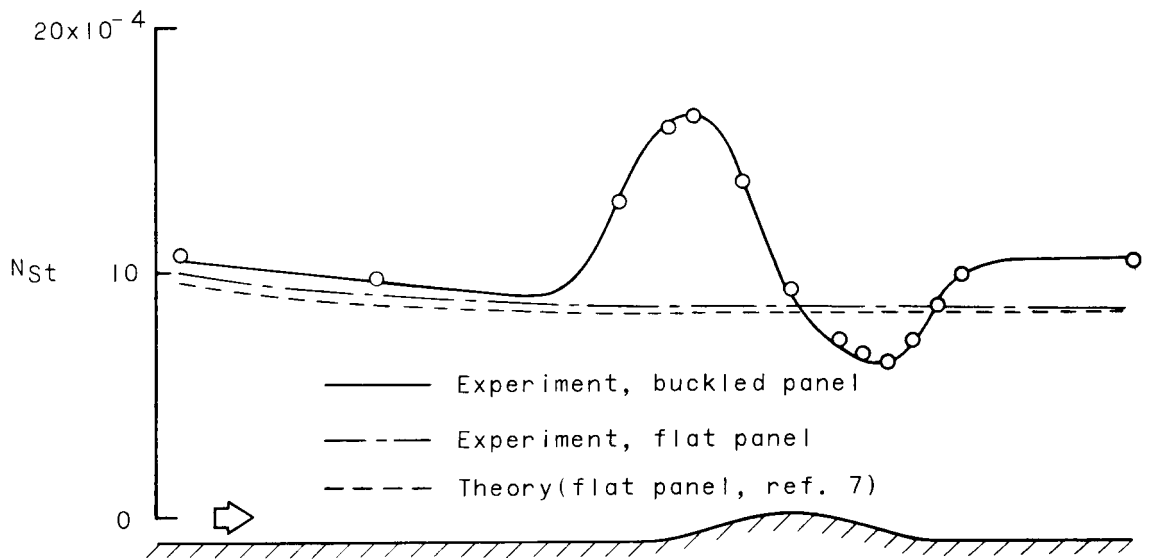


(b) Panel 8A.

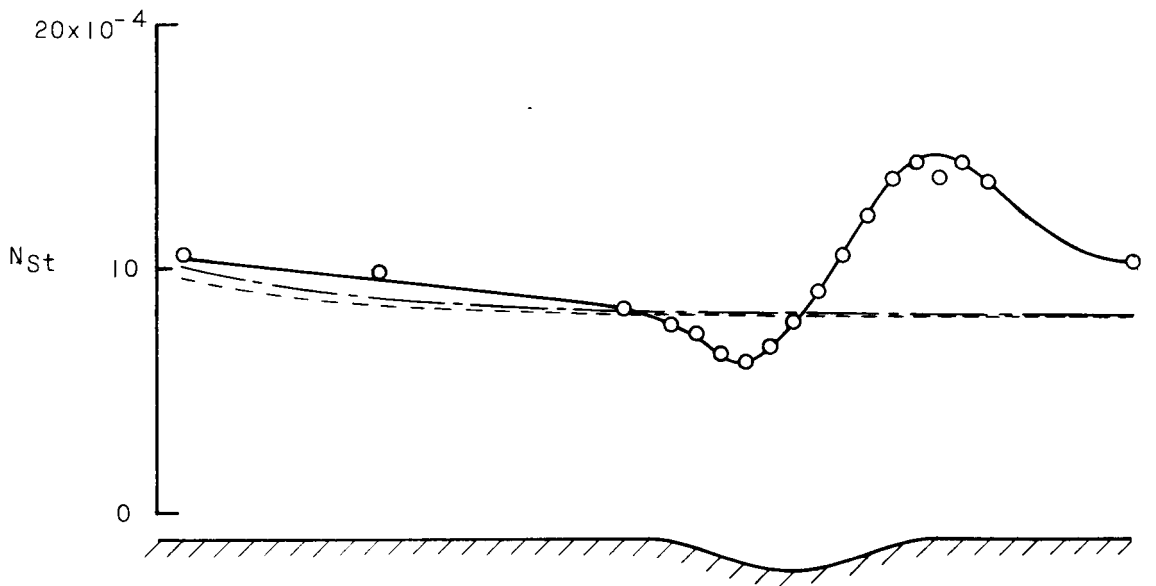


(c) Panel 9A.

Figure 9.- Center-line pressure-coefficient distributions. Reynolds number at leading edge of buckle approximately 48×10^6 . Arrow indicates direction of flow.

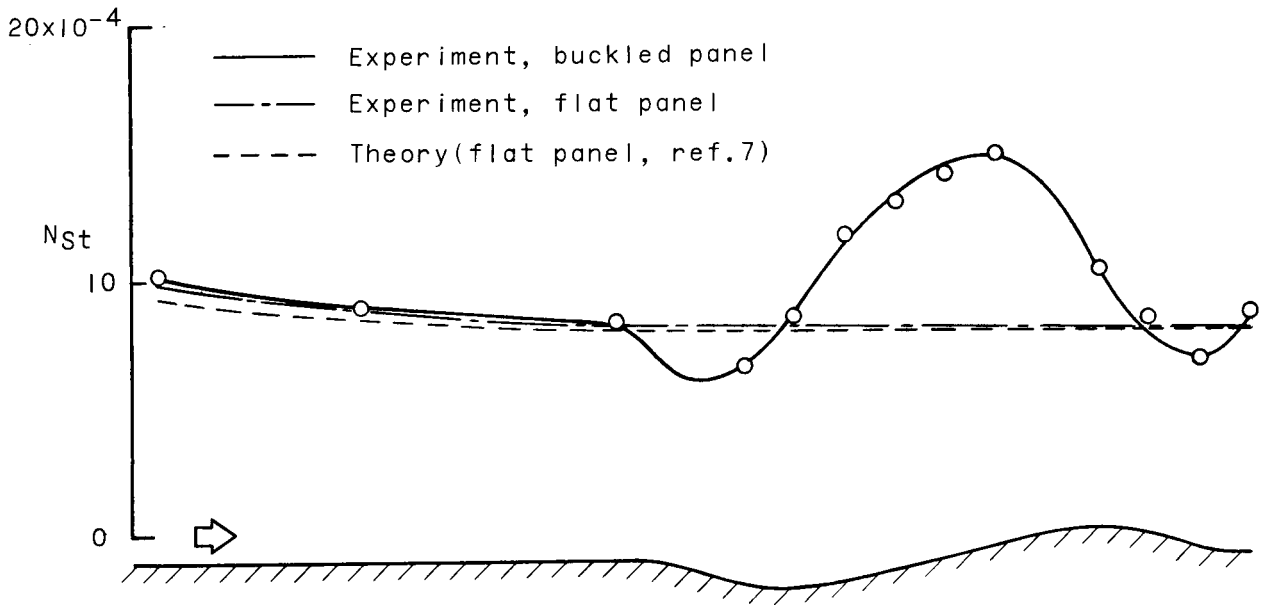


(a) Single buckle out. $\frac{h_{b,max}}{l} = 0.091$.

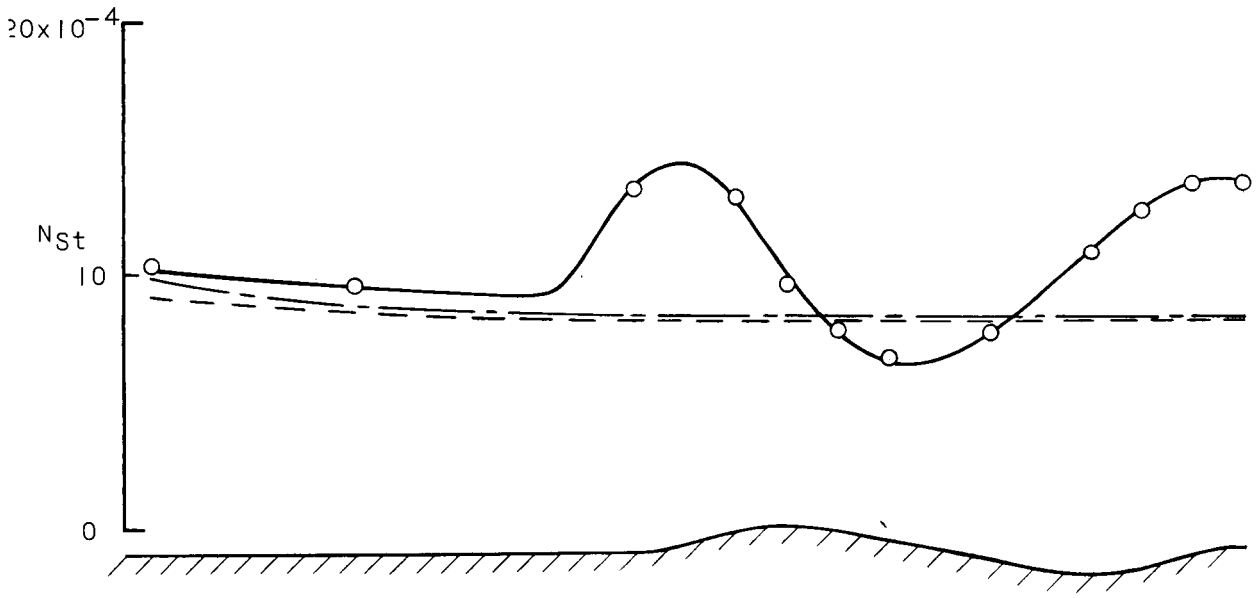


(b) Single buckle in. $\frac{h_{b,max}}{l} = 0.098$.

Figure 10.- Center-line Stanton number distributions. Arrow indicates direction of flow.



(c) Double buckle, in-out. $\frac{h_{b, \max}}{\lambda} = 0.099$ and 0.093 .



(d) Double buckle, out-in. $\frac{h_{b, \max}}{\lambda} = 0.082$.

Figure 10.- Concluded.

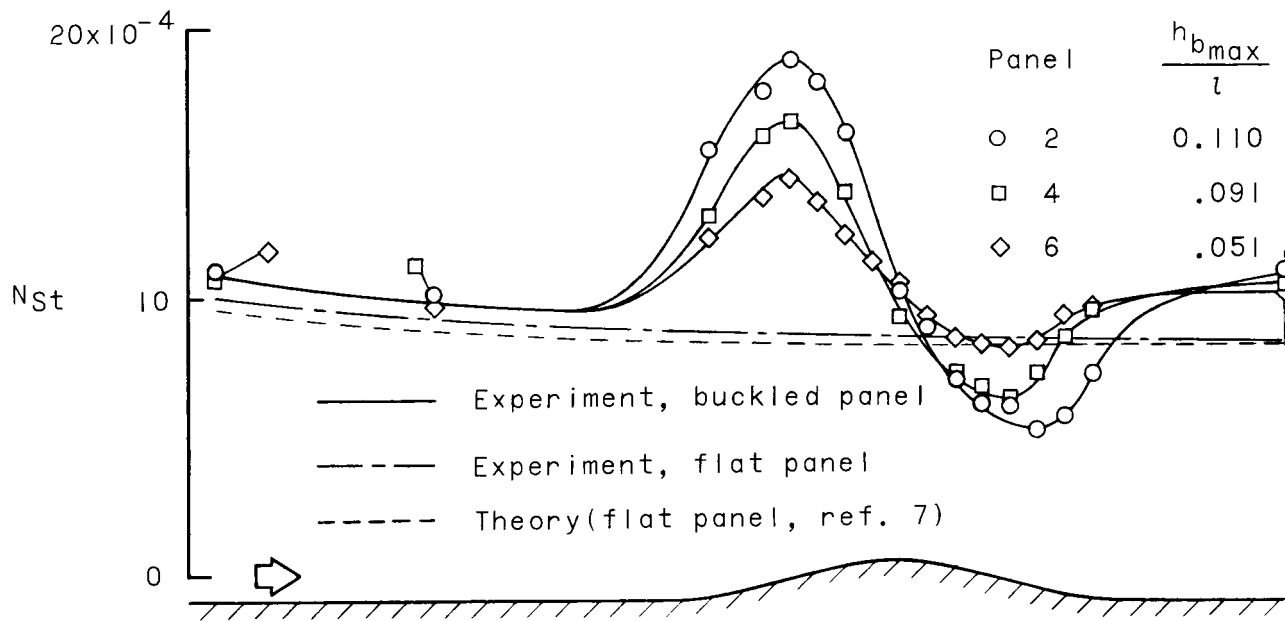


Figure 11.- Summary plot of center-line Stanton number distributions for 6-inch, buckle-out panels.

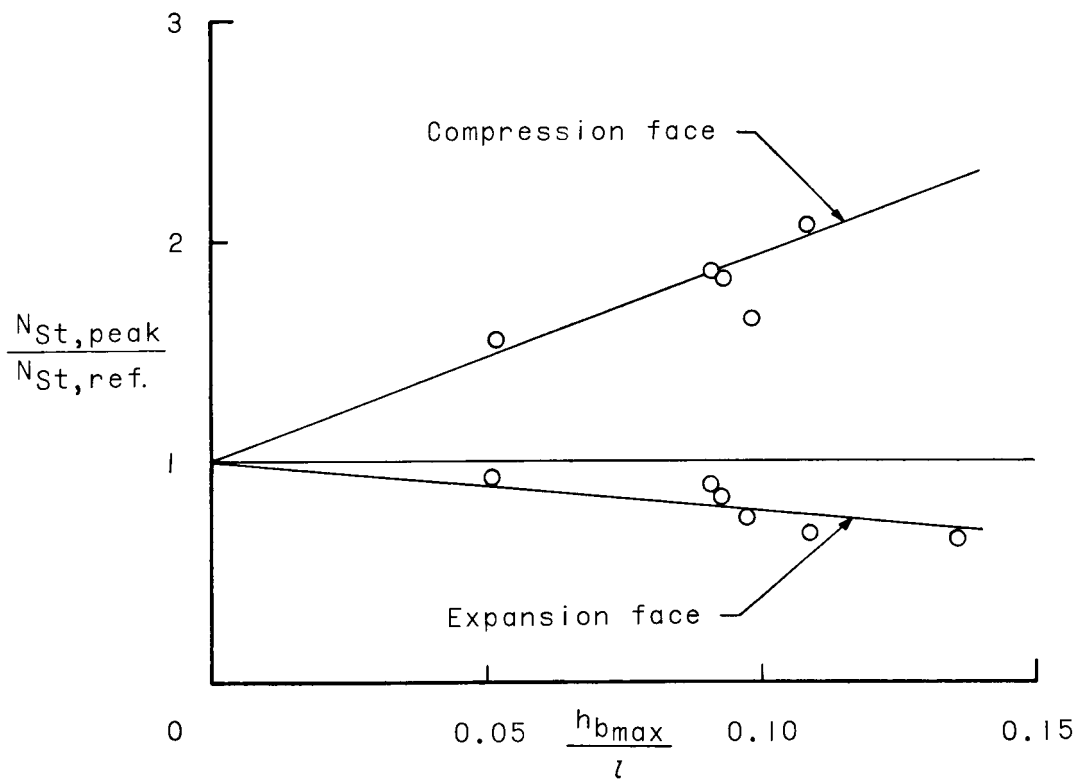


Figure 12.- Correlation plot for single-buckle panels of variation in peak Stanton numbers with buckle size.